Short Communication

Preparation and Electrochemical Properties of LiMn₂O₄ by Solid-State Combustion Synthesis Method Using Starch as a Fuel

Qiling Li[1,2], Cancan Peng[1,2], Jijun Huang[1,2], Wangqiong Xu[1,2], Fangli Yang[1,2], Hongli Bai[1,2], Changwei Su[1,2], Junming Guo[1,2,]*

[1]Key Laboratory of Resource Clean Conversion in Ethnic Regions，Education Department of Yunnan, Yunnan Minzu University, Kunming 650500, PR China
[2]Joint Research Centre for International Cross-border Ethnic Regions Biomass Clean Utilization in Yunnan, Yunnan Minzu University, Kunming 650500, PR China
[*]E-mail: guojunming@tsinghua.org.cn

Spinel LiMn₂O₄ cathode materials were prepared by solid-state combustion synthesis using manganese carbonate, lithium carbonate as raw materials and starch as a fuel. The powders of LiMn₂O₄ were characterized by X-ray diffraction (XRD) and scanning electron micrographs (SEM). The influence of the starch content (0-30 wt.%) on products' discharge capacity and electrochemical characteristic properties in terms of cycle performance were also analyzed by galvanostatic charge-discharge test and cyclic voltammetry (CV). XRD pattern indicate that all the LiMn₂O₄ powders are a single-phase crystal. Cyclic voltammograms showed two reversible processes, which is the topical response of LiMn₂O₄, the electrochemical performance demonstrates that all the specific capacity and capacity retention of the sample with different amounts of starch additive are improved.

1. INTRODUCTION

The lithium manganese oxide LiMn₂O₄ of spinel structure has been regarded as one of the most promising cathode materials for lithium-ion batteries due to its advantages such as an abundant of raw materials, cheap resources, environment-friendliness and easy of preparation. So it has been extensively investigated as a cathode material for lithium-ion batteries [1-5].

It was found that the electrochemical properties of $LiMn_2O_4$ are strongly influenced by the synthesis methods. Many approaches, such as solid-state reaction [6], sol-gel method [7], the combustion synthesis [8] and so on have been developed to prepare $LiMn_2O_4$. Among these techniques, a novel solid-state combustion synthesis method, based on solid-state and combustion reaction, has attracting extensive interest because it can save reaction time and energy at the same time compared the conventional solid-state and combustion reaction [9].

Our research group has successfully synthesized the spinel $LiMn_2O_4$ via solid-state combustion synthesis [9-11]. We found that different organic fuels have an impact on its electrochemical performance of spinel $LiMn_2O_4$. Because the combustion heat value varies with the type of organic fuel, starch and oxalic acid will have an influence on the micromorphology and electrochemical performance of $LiMn_2O_4$. But as far as we know, the $LiMn_2O_4$ products prepared by solid-state combustion synthesis using starch as fuel was ralely not reported. In this paper, the $LiMn_2O_4$ was successfully synthesized via solid-state combustion synthesis, Additional heat can be released during the combustion of starch, and improved system temperature leads to a more rapidly reaction rate. In order to explore the effect of starch content on the electrochemical performance of $LiMn_2O_4$, different amount of starch (0, 10, 20, 30 wt.%) were chosen as the research object.

2. EXPERIMENT

2.1 Material preparation

The powder of $LiMn_2O_4$ was prepared by the novel solid-state combustion synthesis using starch (AR, Tianjin No.3 Chemical Reagent Factory) as a fuel. The carbonates of Li_2CO_3 and $MnCO_3$ (Sinopharm Chemical Reagent Co., Ltd.,) were used as lithium and manganese source. Firstly, stoichiometric mounts of Li_2CO_3 and $MnCO_3$ were weighted based on atomic ratio of Li:Mn=1:2, then put into a 500 mL polytetrafluoroethylene jar. 0, 10, 20, 30 wt.% starch together with ethanol were also added into the jar. Secondly, the total raw materials and fuel were ball-milld thoroughly by planetary ball mill for 8 h to make the reagents dispersed homogeneously and then dried in the oven at 80 ^{o}C to evaporate the ethanol. Finally the precursor was ground and combusted in a muffle furnace at 600 ^{o}C for 1 h in air, after taken out and cooled down to ambient temperature naturally the products were obtained.

2.2 Materials characterization

The crystal structure of the materials was measured by X-ray diffraction (XRD, DMax-TTRⅢ, Japan) using Cu Kα radiation, the scanning range of diffraction angle (2θ) was 10-70°, The scanning rate was 4° min^{-1} and step width of 0.02^o with 30 mA operation current and 40 kV voltage, lattice parameters were obtained using Jade 5.0 software. The morphology of the samples were observed using a scanning electron microscopy (SEM, QUANTA 200, America FEI).

2.3. Electrochemical measurements

Electrochemical properties of as-prepared powders were measured with CR-2025 coin-type cells. The electrodes were fabricated by mixing the active materials powder, conductive carbon, and polyvinylidene fluoride in a weight ratio of 8:1:1 in N-methylpyrrolidinone solvent. Then the mixture was spread onto aluminum foil and dried at 120 ^{o}C for 12 h. The cells consisted of the as- fabricated electrodes as the positive, metallic lithium as the counter electrodes, polypropylene film (Celgard 2320) separator, and the electrolyte consisted of 1 mol/L $LiPF_6$ in ethylene carbonate and dimethyl carbonate (volume ratio=1:1). Cell fabricated in an argon-filled glove box. The galvanostatic charge and discharge tests of the cells were performed at a current density of 0.2 C within the 3.2-4.35 V (versus Li/Li$^+$) potential range on an CT2001A battery testing system (Wuhan Jinnuo Electronics Co., Ltd., China). Cyclic voltammetry (CV) was performed on an electrochemical workstation (IM6ex, ZAHNER-Elektrik GmbH & Co. KG, Germany). The CV curves were recorded at a scan rate of 0.2 mV s^{-1} between 3.2 and 4.35 V (versus Li/Li$^+$).

3. RESULTS AND DISCUSSION

3.1. Structural and morphological characterization
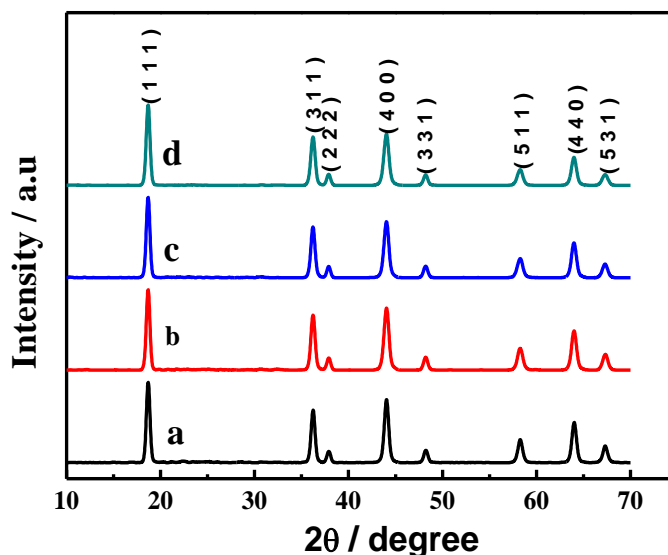
Figure 1. XRD pattern of the samples obtained for the different contents of starch:(a) 0, (b) 10 wt.%, (c) 20 wt.%, (d) 30 wt.% starch, respectively.

Fig. 1 shown the XRD pattern of the samples obtained for the different contents of starch calcined at 600 ^{o}C for 1 h. All of the main diffraction peaks can be indexed by the cubic spinel structure of $LiMn_2O_4$ (JCPDS NO. 35-0782) with space group of Fd3m, corresponding to the eight crystal planes of (1 1 1), (3 1 1), (2 2 2), (4 0 0), (3 3 1), (5 1 1), (4 4 0), and (5 3 1), where Li ions occupy in tetrahedral sites (8a), Mn atoms in octahedral sites (16d) and O^{2-} ions is located at octahedral

sites (32e) [12].The variation of the lattice parameters for $LiMn_2O_4$ obtained for the different contents of starch is show in table 1.

Table 1. Lattice parameters for $LiMn_2O_4$ obtained for the different contents of starch

Fuel amount (wt%)	Lattice parameters (Å)
0	8.22164
10	8.22044
20	8.22051
30	8.22091

The lattice parameters increases with starch additive, because of the increased amount of starch, additional heat can be released during the combustion of starch, and improved system temperature. Mn ions are present in the Mn^{4+} state due to the more stability of Mn^{4+} at low temperature [13], so,the radius of Mn^{4+} (0.60 Å) is smaller than Mn^{3+} (0.68 Å) [14], result in declined values of lattice parameters.
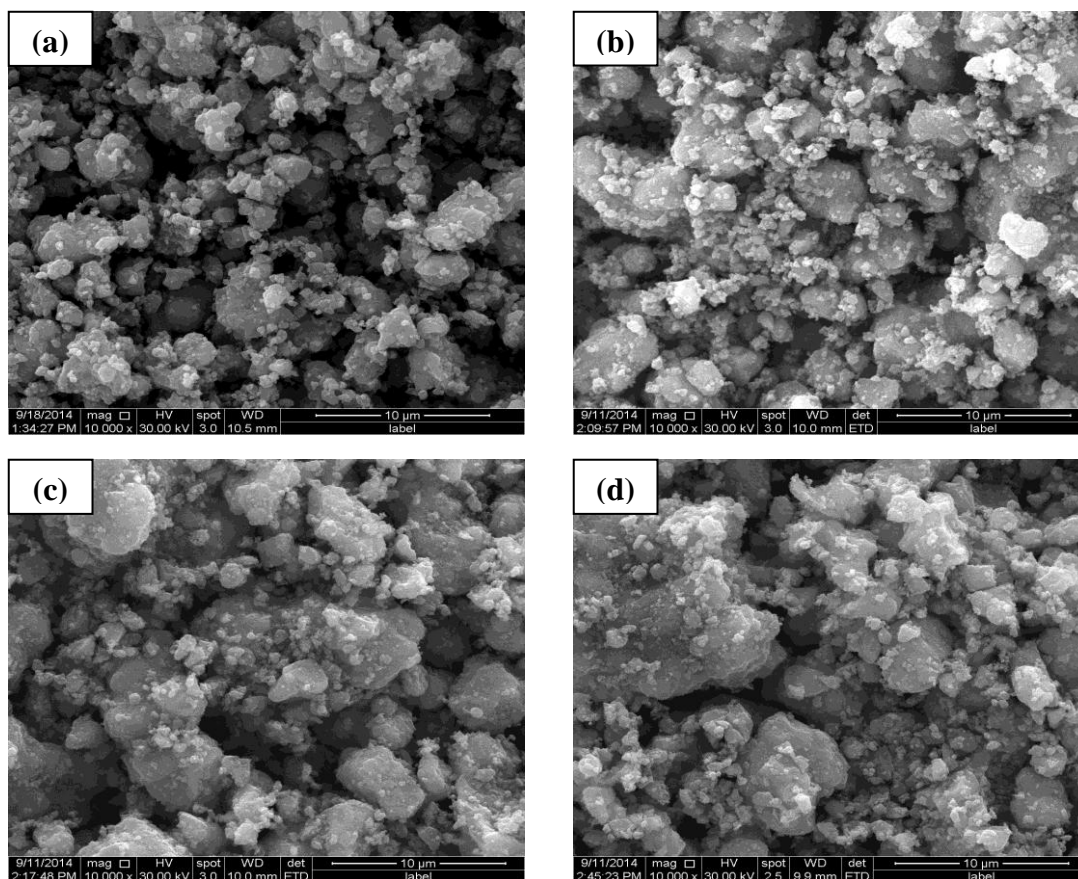
Figure 2. SEM images of the samples obtained for the different contents of starch:(a) 0, (b) 10 wt. %, (c) 20 wt. %, (d) 30 wt. % starch, respectively.

Fig 2. displays the SEM images of $LiMn_2O_4$ prepared by solid-state combustion synthesis using starch as a fuel. It is obvious that all the samples distributed un-uniformly and the large particles surfaces covered with some small grains. With the increase of starch content, the particle size increases and the agglomeration becomes more seriously. Among them, the particle size of sample without fuel is about between 1.1 and 3.2 μm, after different contents of starch were added (b-d), the grains size distribution ranges from 1.5 to 5.2 μm, indicating that the grains size is influenced by the content of starch.

3.2 Electrochemical performance of as-prepared $LiMn_2O_4$
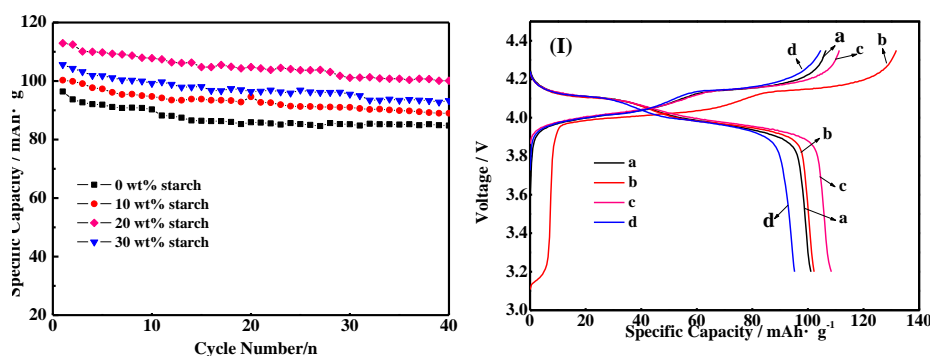
Figure 3. (I) The initial charge/discharge curves and (Π) the cycling performance curves of the samples at 0.2 C obtained for the different contents of starch:(a) 0, (b) 10 wt.%, (c) 20 wt.%, (d) 30 wt.% starch, respectively, at room temperature.

Fig. 3 (I) exhibits the initial charge/discharge curves and (Π) the cycling performance curves of the samples between 3.2 and 4.35 V at 0.2 C obtained for the different contents of starch:(a) 0, (b) 10 wt.%, (c) 20 wt.%, (d) 30 wt.% starch, respectively, at room temperature. The data of initial, 40th discharge capacities, and capacity retention of products are summarized in table 2.

Table 2. Initial, 40th discharge capacities, and capacity retention of the samples obtained for the different contents of starch:(a) 0, (b) 10 wt.%, (c) 20 wt.%, (d) 30 wt.% starch, respectively.

Fuel amount (wt%)	Discharge capacity (mAh g^{-1})		capacity retention (%)
	1st	40th	
0	96.3	84.8	88.0
10	100.3	89	88.7
20	112.9	100.1	88.7
30	105.6	93.3	88.4

It can be observed that all the initial charge/discharge curves clearly display two voltage plateaus in the potential region of 3.9-4.2 V, indicating a two-step lithium deintercalation/intercalation

process in spinel $LiMn_2O_4$ [15]. The product without starch delivers a slightly lower initial discharge capacity of 96.3mAh g^{-1}, however, the products with 10, 20 and 30 wt. % starch deliver relatively high initial discharge capacity of 100.3, 112.9 and 105.6 mAh g^{-1}, respectively. After 40 cycles sample (a) with the retention of 84.8 %, sample (b), (c) and (d) with the retention of 88.7 %, 88.7 % and 88.4 %, respectively. As can be seen from the results, the products of initial discharge capacities increases when the contents of starch increases to 20 wt.% firstly, and then decreases when more starch is added. Sample (c) prepared with 20 wt.% starch display the highest initial discharge capacity of 112.9 mAh g^{-1}, so the optimal content of starch is 20 wt.%. The $LiMn_2O_4$ prepared with 5 wt% oxalic acid by solid-state combustion synthesis method present a a relatively low initial discharge capacity of 108.5 mAh g^{-1} [11]. Using starch as a fuel can obtain $LiMn_2O_4$ with a higher initial discharge capacity compared with oxalic acid.

3.3 CV analysis
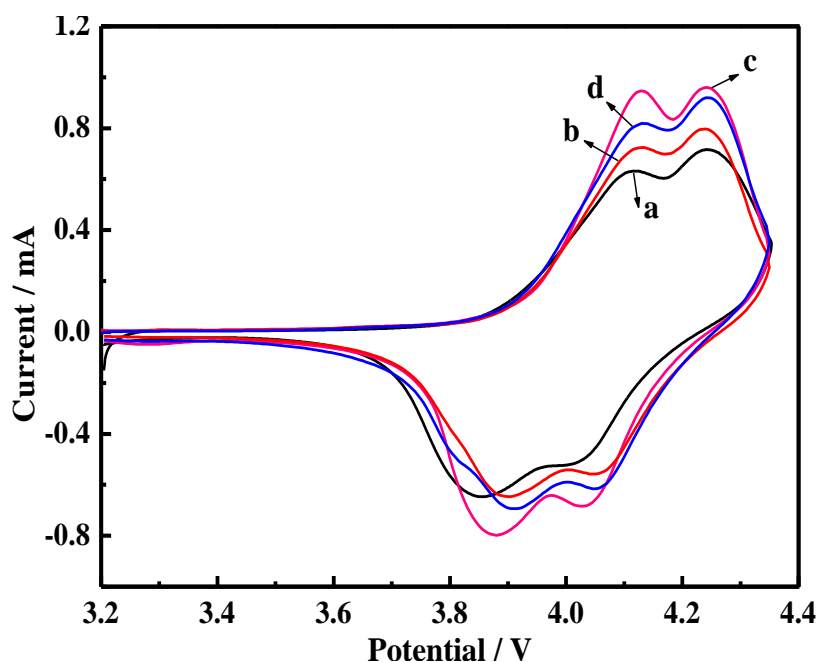
Figure 4. CV of the samples obtained for the different contents of starch:(a) 0, (b) 10 wt.%, (c) 20 wt.%, (d) 30 wt.% starch, respectively.

Fig. 4 exhibits the CV of the samples obtained for the different contents of starch: (a) 0, (b) 10 wt.%, (c) 20 wt.%, (d) 30 wt.% starch in the potential range of 3.2-4.35 V at a scan rate of 0.2 mV s^{-1} at room temperature. It can be observed that all the cyclic voltammograms curves clearly display two pairs of reversible redox peaks in the potential region of 3.80-4.30 V, correspond to deintercalation/intercalation of lithium from the spinel $LiMn_2O_4$ is a two-step process [16], the results are agreement with the initial charge/discharge curves (I) . Sample (c) displays the highest current peaks, it can be draw a conclusion that the materials prepared with 20 wt.% starch processes the highest initial discharge capacity.

4. CONCLUSIONS

$LiMn_2O_4$ powders were successfully synthesized via a solid-state combustion synthesis using starch as a fuel at 600 ^oC. With the use of starch a single-phase of $LiMn_2O_4$ can be obtained in a short time, results of this study display that the micromorphology and electrochemical performance of products were affected by the content of starch. The particle sizes increase with the increase of starch content, all the specific capacity and capacity retention of the sample with different amounts of starch additive are improved. The $LiMn_2O_4$ materials obtained with 20 wt.% starch display a highest initial discharge capacity of 112.9 mAh g^{-1} and the capacity retention of 88.7% after 40 cycles compared with other contents, the $LiMn_2O_4$ obtained with 0 wt.% starch delivers a slightly lower initial discharge capacity of 96.3mAh g^{-1} and the capacity retention of 88.0% after 40 cycles. It is believed that this method would be easily extended to large-scale production, which saves reaction time and energy at the same time.

Reference

1. Y.J. Wei, K.B. Kim, G. Chen and C.W. Park, *Mater. Charact*. 59 (9) (2008) 1196–1200.
2. R. Vidu and P. Stroeve. Ind. Eng, *Chem. Res*. 43 (13) (2004) 3314–3324.
3. D. W. Chung, N. Balke, S.V. Kalinin and R. Edwin Garcia, *J. Electrochem. Soc*., 158 (10) (2011) A1083–A1089.
4. G. Amatucci and J.M. Tarascon, *J. Electrochem. Soc*., 149 (12) (2002) K31–K46.
5. X.M. He, J.J. Li, Y. Cai, Y.W. Wang, J.R. Ying, C.Y. Jiang and C.R. Wan, *J. Solid State Electrochem*., 9 (6) (2005) 438–444.
6. C.H. Zheng, X. Liu, Z.F. Wu, Z.D. Chen and D. L. Fang, *Electrochim. Acta*., 111 (2013) 192–199.
7. Wang. SJ, Li.P, Shao. LY, Wu. KQ, Lin. XT, Shui. M, Long. NB, Wang. DJ and Shu. J, *Ceram Int*. 41 (2015) 1347–1353.
8. Chunyu Zhu, Akira Nobuta, Genki Saito, Isao Nakatsugawa and Tomohiro Akiyama, *Adv Powder Technol*. 25 (2014) 342–347.
9. Xianyan Zhou, Mimi Chen, Hongli Bai, Changwei Su, Lili. Feng and Junming. Guo, *Vacuum*. 99 (2014) 49-55.
10. Xianyan Zhou, Mimi Chen, Mingwu Xiang, Hongli Bai and Junming Guo, *Ceram Int*. 39 (2013) 4783-4789.
11. Cancan Peng, Hongli Bai, Qiling Li, Yujiao Guo, Jijun Huang, Changwei Su and Junming Guo. *Int. J. Electrochem. Sci*., 10 (2015) 3885 - 3896.
12. P. Arora, B.N. Popov and R.E. White, *J. Electrochem. Soc*. 145 (1998) 807-815.
13. Christian Masquelier, Mitsuharu Tabuchi, Kazuaki Ado, Ryoji Kanno, Yo Kobayashi, Yuzuru Maki, Osamu Nakamura and John B. Goodenough, *J. Solid State Chem*. 123 (1996) 255-266.
14. W. Borchardt-Ott, Crystallography, *Springer*, New York, 1993.
15. W.J. Zhou, S.J. Bao, Y.Y. Liang, B.L. He and H.L.Li. *J. Solid State Electrochem*., 10 (2006) 277-282.

16. Z.h. Li, J. Yang, J.L. Wang, J.J. Tang, G.T. Lei and Q.Z.Xiao. *Microporous Mesoporous Mater*. 162 (2012) 44-50.